Published in final edited form as:
Exp Neurol. 2014 January ; 251: 84–90. doi:10.1016/j.expneurol.2013.11.005.

Targeting deficiencies in mitochondrial respiratory complex I and functional uncoupling exerts anti-seizure effects in a genetic model of temporal lobe epilepsy and in a model of acute temporal lobe seizures

Kristina A Simeone, PhD[1,*], **Stephanie A Matthews, MA**[1], **Kaeli K Samson, MA**[1], and **Timothy A Simeone, PhD**[1]

[1]Pharmacology Department, Creighton University School of Medicine, Omaha, Nebraska, USA, 68178

Abstract

Mitochondria actively participate in neurotransmission by providing energy (ATP) and maintaining normative concentrations of reactive oxygen species (ROS) in both presynaptic and postsynaptic elements. In human and animal epilepsies, ATP-producing respiratory rates driven by mitochondrial respiratory complex (MRC) I are reduced, antioxidant systems are attenuated and oxidative damage is increased. We report that MRCI-driven respiration and functional uncoupling (an inducible antioxidant mechanism) are reduced and levels of H_2O_2 are elevated in mitochondria isolated from KO mice. Experimental impairment of MRCI in WT hippocampal slices via rotenone reduces paired-pulse ratios (PPRs) at mossy fiber-CA3 synapses (resembling KO PPRs), and exacerbates seizure-like events *in vitro*. Daily treatment with AATP [a combination therapy composed of ascorbic acid (AA), alpha-tocopherol (T), sodium pyruvate (P) designed to synergistically target mitochondrial impairments] improved mitochondrial functions, mossy fiber PPRs, and reduced seizure burden index (SBI) scores and seizure incidence in KO mice. AATP pretreatment reduced severity of KA-induced seizures resulting in 100% protection from the severe tonic-clonic seizures in WT mice. These data suggest that restoration of bioenergetic homeostasis in the brain may represent a viable anti-seizure target for temporal lobe epilepsy.

Keywords

Mitochondria; seizures; epilepsy; kainic acid; Kv1.1 knockout mice; Kcna1-null mice; ascorbic acid; pyruvate; alpha-tocopherol; mitochondrial uncoupling; mitochondrial complex I; paired-pulse ratios; seizure-like events; ROS; antioxidant; field potentials

* Corresponding Author Kristina Simeone, PhD Assistant Professor Creighton University School of Medicine Department of Pharmacology Criss III Room 551 2500 California Plaza Omaha, NE 68178 Office: 402-280-2734 Fax: 402-280-2142.

Potential Conflict of Interest:
The authors report a patent pending concerning the formulation of AATP and use as an anti-seizure therapeutic.

INTRODUCTION

Mitochondria are active participants in neurotransmission directly providing energy (ATP), sequestrating calcium and maintaining normative concentrations of reactive oxygen species (ROS) in both presynaptic and postsynaptic elements of the synapse (Ligon and Steward, 2000; Thiels et al., 2000; Knapp and Klann, 2002; Kamsler and Segal, 2003a; Hongpaisan et al., 2004; Guo et al., 2005; Kann et al., 2011; Massaad and Klann, 2011; Chouhan et al., 2012; Hall et al., 2012; Harris et al., 2012). In human epilepsies and animal models in which seizures are induced with the chemoconvulsant kainic acid (KA), deficiencies of brain mitochondria are prevalent and include reductions in the activity of ATP-producing mitochondrial respiratory complex I (MRCI), diminished antioxidant systems (including functional uncoupling), and increased oxidative damage (Wallace, 1992; Bruce and Baudry, 1995; DiMauro et al., 1999; Kunz et al., 2000; Mueller et al., 2001; Sudha et al., 2001; Sullivan et al., 2003; Malthankar-Phatak et al., 2006; Jarrett et al., 2008; Vielhaber et al., 2008; Kudin et al., 2009; Ryan et al.,, 2012). The chronic nature of these dysfunctions and the role of mitochondria in neurotransmission raise the possibility that ‘pathologic’ mitochondria may contribute to a negative feedforward mechanism that exacerbates network hyperexcitability.

Here, we report similar deficiencies in cortical and hippocampal mitochondria isolated from epileptic Kv1.1 knockout (KO) mice, an idiopathic model that is clinically relevant to several human epilepsy syndromes (Wenzel et al., 2007; Fenoglio-Simeone et al., 2009; Simeone et al., 2013), and demonstrate that acutely inhibiting MRCI in wild-type (WT) hippocampal slices reduces mossy fiber-CA3 PPRs and exacerbates epileptiform activity *in vitro*.

We designed a treatment to test the hypothesis that synergistically targeting mitochondrial impairments exerts anti-seizure effects in epileptic KO mice and against acute KA-induced seizures. The combination treatment is composed of Ascorbic Acid, alpha-Tocopherol, and sodium Pyruvate (referred to as AATP). Sodium pyruvate enhances ATP-producing MRCI functions as an MRCI anaplerotic substrate that is preferred over glucose oxidation during conditions of low ATP levels (Kovac et al., 2012), and can be converted to fatty acids to enhance mitochondrial uncoupling. Pyruvate may aid in restoring energy sources and attenuating the increase in lactate/pyruvate ratios, which have been reported during seizures (Kawai et al., 2006). Ascorbic acid and alpha-tocopherol are scavengers of oxidizing radicals that also exert cooperative redox interactions (Chaudière, and Ferrari-Iliou, 1999). Alpha-tocopherol is also involved in increasing levels of the antioxidant catalase and free fatty acids, enhancing functional uncoupling via peroxisome proliferator-activated receptor gamma activation, and promoting mitochondrial biogenesis (Munteanu et al., 2006; Lian et al., 2007; Wu et al., 2009; Yonutas and Sullivan, 2013). We report that daily AATP treatment improved mitochondrial respiration and functional uncoupling, reduced ROS levels, restored hippocampal PPRs and significantly attenuated seizure burden in KO mice. In addition, pretreatment with AATP protected WT mice from severe acute KA-induced seizures.

MATERIALS AND METHODS

Animals

C3HeB/FeJ Kcna1-null (Kv1.1 knockout, KO) and wild-type (WT) mice were reared on a 12hr light/dark cycle with ad libitum access to food and water. All experiments conformed to NIH guidelines in accordance with the United States Public Health Service's Policy on Humane Care and Use of Laboratory Animals and were approved by Creighton University's Institutional Animal Care and Use Committee.

Mitochondrial isolation and oxygen polarography

Mice were anesthetized with isoflurane and cortical and hippocampal tissues were quickly micro-dissected on ice. Tissue was homogenized in isolation buffer (5×V/V in mM: 215 mannitol, 75 sucrose, 1 EGTA 20 HEPES and 0.1% BSA, pH 7.2 adjusted with KOH) and mitochondria were isolated using differential centrifugation as we have described (Brown et al., 2004). Isolated mitochondria were resuspended in isolation buffer without EGTA. Protein concentrations were determined with Bradford's assay. Mitochondria (100 μg) were resuspended in KCl respiration buffer (in mM: 125 KCl, 20 HEPES, 2 $MgCl_2$, 2.5 KH_2PO_4, pH 7.2) and placed in a sealed, thermostatically controlled chamber at 37°C. Oxygen polarography was measured using a standard Clark-type electrode (Hanstech Instruments, Ltd., Norfolk, England) as we have described (Sullivan et al., 2003, 2004). The following sequential parameters were measured in duplicates per sample (see Fig.1A): Mitochondria were energized via ATP-producing NADH:coenzyme Q oxidoreductase (complex I)-driven state III respiration with 5 mM pyruvate and 2.5 mM malate (PM) and concurrent activation of adenosine triphosphate (ATP) synthase by 150 μM adenosine diphosphate (ADP); state IV respiration was initiated with oligomycin- (oligo-) induced inhibition of ATP synthase (1 μM); maximal respiratory rate (state V) was measured in the presence of the chemical protonophore p-triflourometh-oxyphenylhydrazone (FCCP; 1 μM); and MRCI-respiratory dependency was verified in the presence of the MRCI inhibitor rotenone (Rot). Oxygen consumption in the presence of 100 and 400 μM H_2O_2 was determined in energized mitochondria following stabilization of the ADP response. Functional uncoupling was determined in energized mitochondria following application of free fatty acids (FA, 300 μM palmitate) in state IV (with oligo) as we have described (Sullivan et al., 2004). Uncoupling was reversed via chelation of fatty acids with BSA. Only samples with a respiratory control ratio that was greater than 4 were analyzed. Unbiased assessment of the rate of oxygen consumption was determined using computer-generated line of best-fit algorithm and nmol of oxygen mg^{-1} min^{-1} was calculated.

Spectrofluorometric analysis of H_2O_2

Levels of ROS, specifically H_2O_2, were assessed in energized mitochondria following 30 min incubation on ice with dichlorofluorescein, using a BioTek Synergy Microplate Reader (BioTek, Winooski, VT) at 37°C, as we have described (Sullivan et al., 2003). Samples were run in duplicates. Relative fluorescent units (Fmax/Fmin) in the presence of oligomycin were normalized within sample to values of mitochondria alone.

Immunofluorescent western blots

To probe for mitochondrial proteins, lysed isolated mitochondria (20 μg) were heated to 37°C for 5 min, ran through a 4-20% TGX pre-cast gel (Biorad, Hercules, CA), transferred to a fluorescent appropriate membrane (Immobilon-Fl; Millipore, Billerica, MA) and blocked using a 1:1 PBS to Odyssey's blocking buffer (Licor, Lincoln, NE). Mitochondrial respiratory complexes (MRC) I-V proteins [MRCI: NDUFB8 subunit, II: 30kDa, III: core protein 2, IV: subunit I, and V: alpha subunit] were simultaneously determined with MitoProfile Total OXPHOS cocktail primary (1:1000; MS604, MitoSciences, Eugene, OR). Uncoupling protein 2 (UCP2) was probed using lysed isolated mitochondria (heated to 99°C), ran through the precast gel, transferred and blocked. Rabbit anti-UCP2 (1:100; AB3042, Millipore, Billerica, MA) and mouse anti-VDAC (housekeeping gene, 1:80,000; 73-204, Neuromab, Davis, CA) were used. After overnight incubation, the membranes were probed with the appropriate fluorescent secondaries secondary antibodies (IRDye 680 or IRDye 800CW; Licor, Lincoln, NE). WT and KO samples were run in duplicate on each gel. Densitometric analysis was conducted using images captured on an Odyssey FC (Licor, Lincoln, NE). Averages of the duplicates were determined and normalized to the WT values within each gel.

Acute slice preparation and multi-electrode array recordings

Acute hippocampal slices were prepared and multi-electrode array recordings were conducted as we have described (Simeone et al., 2011, 2013). Briefly, mice (P30-P40) were anesthetized with isoflurane, decapitated, and their brains removed and quickly placed into ice cold, oxygenated (95%O2/5%CO2) cutting artificial cerebrospinal fluid (aCSF) containing (in mM): 206 Sucrose, 2.8 KCl, 1 CaCl2, 1 MgCl2, 2 MgSO4, 26 NaHCO3, 1.25 NaH2PO4, and 10 glucose (pH 7.4). Horizontal sections (350 μM) were cut and transferred to a holding chamber for 1 hr with warm (32°C) oxygenated aCSF containing (in mM): 125 NaCl, 3.0 KCl, 2.0 CaCl2, 1.3 MgSO4, 26 NaHCO3, 1.25 NaH2PO4, and 10 glucose (pH 7.4). Slices were placed on a multi-electrode array (MED64 system, Alpha Med Systems, Osaka, Japan). A custom probe cap allowed delivery of humidified air (95%O2/5%CO2) and perfusion (1 ml min-1) of in-line pre-warmed oxygenated aCSF. The bath level was maintained near interface. Rotenone (100 nM) or DMSO vehicle (0.01%) in aCSF was bath applied for 60 min during which paired stimulations of the hilus (50 msec interval, intensity set at 50% maximal response) were performed every 90 sec. Following completion of the stimulation protocol, high potassium (8 mM) aCSF with either rotenone or vehicle was perfused for 90 min to elicit seizure-like events (SLEs). Evoked and spontaneous events were recorded with Mobius v2 (Witwerx Inc., Tustin, CA, USA) software and acquired at a 20 kHz sampling rate with a bandwidth of 0.1 Hz–10 kHz. Evoked data were analyzed in Mobius v2. Input-Output (I/O) relationships of raw and normalized data were fit with a Boltzmann equation to obtain stimulation intensities eliciting 50% of the maximum response (V50) using Prism 6 software (Graphpad Software, Inc., La Jolla, CA, USA). Spontaneous data were imported into Spike2 v7 software (Cambridge Electronic Design, Cambridge, England) for analysis.

Electroencephalography electrode implantation surgery and seizure scoring

Mice were maintained under isoflurane anesthesia and normothermic conditions. One ground (1.5mm anterior lamba, 1.5mm lateral) and two subdural (1mm posterior Bregma, 1.5mm bilateral) cortical electro-encephalographic (EEG) electrodes were implanted, secured and attached to a headmount. Following a 5-7 day recovery, seizures were monitored using continuous infrared video surveillance system time-linked to EEG technology (Pinnacle Technology, Inc.) as we have described (Fenoglio-Simeone et al., 2009). During seizure monitoring, mice were single-housed in hexagon cages. EEG seizures were identified using Pinnacle 8400 software and behavioral manifestations were manually verified with time-stamped video recordings.

AATP pretreatment and acute KA induced seizures in WT mice

Adult WT mice were pretreated with AATP [two i.p. injections: ascorbic acid (250mg/kg) and sodium pyruvate (500mg/kg) in saline immediately followed by alpha-tocopherol (30mg/kg) in ethanol] or two matched volume vehicle injections. Thirty minutes following pretreatment, KA was administered (15mg/kg, i.p.). Seizure severity was scored every 5 min for three hours using a modified Racine scale (Fenoglio-Simeone et al., 2009): 0-normal; 1-immobility; 2-head bobbing; 3-forelimb/hindlimb clonus, tail extension, a single rearing event; 4-continuous rearing and falling; 5-severe tonic-clonic seizures. The most severe seizure per 30 min epoch was recorded and plotted. Seizure burden index (SBI) scores of the acute seizures were generated using the following equation: $SBI = [\Sigma(\sigma_i)]/\varepsilon$, where σ indicates the most severe seizure; i indicates each stage of seizure (1-5); and ε indicates the total number of epochs scored.

Daily AATP treatment in KO mice

Incidence and severity of each stage seizure was recorded in 1 min epochs for the first 15 min of each hour during the time period of highest seizure occurrence for KO mice (00:00-08:00) (Fenoglio-Simeone et al., 2009). Seizures were monitored and scored in a blinded manner (i) prior to treatment to establish baseline scores (~P21-P24); (ii) during the last two days of the 4-6 day treatment regiment (~P28-29) [treatment consisted of chow enriched in ascorbic acid and alpha-tocopherol (2.5g and 0.30g/kg chow, respectively; Harlan Laboratories, Denver, CO) and sodium pyruvate enriched water (6.67 mg/ml) provided *ad libitum*. Mice consumed 3.4±0.1g chow and 4.4±0.2ml water daily]; and (iii) for 48 hrs following cessation of treatment (during which mice were switched back to standard chow, from ~P30-31). As KO seizure severity and incidence increase with age, seizures were also scored in a cohort of KO controls age-matched to the treatment cessation group (~P31). SBI scores were calculated using the equation: $SBI = [\Sigma(\sigma_i\gamma_i)]/\varepsilon$, where σ indicates the severity; i indicates each stage of seizure (1-5); γ is the incidence; and ε indicates the total number of epochs scored.

Reagents and Statistics

Unless otherwise specified, all reagents were purchased from Sigma. Statistical significance was determined using Student's *t* test or ANOVA with Bonferroni's post hoc test.

RESULTS and DISCUSSION

Cortical and hippocampal mitochondria are 'pathologic' in KO mice

KO mice naturally develop seizures by postnatal day (P) 21 and experience approximately seven daily electro-behavioral seizures that originate in the hippocampus and spread to the cortex (Wenzel et al., 2007; Fenoglio-Simeone et al., 2009). In this idiopathic model, we determined the MRCI-driven respiratory rates in young adult mice (P32-P38) (Fig.1A). ATP-producing state III respiration was diminished by 32±2% in KO cortical and 36±5% hippocampal mitochondria when compared to WT rates (cortical data shown in Fig. 1B, $p<0.05$. Hippocampal KO: 115.2±8.6 vs. WT: 179.9±19.9 nmol O_2 min $^{-1}$mg $^{-1}$, $p<0.05$; n=6-9). The maximal rate of the electron transport (state V) was also reduced to a similar degree in cortical ($p<0.05$, Fig. 1B) and hippocampal mitochondria (hippocampal KO: 193.0±18.2 vs. WT: 312.2±41.2 nmol O_2 min $^{-1}$mg $^{-1}$, $p<0.05$; n=5). These data indicate that mitochondria isolated from KO mice consume less oxygen compared to WT mitochondria despite both groups receiving equivalent concentrations of substrates.

The diminished respiratory rates of KO mitochondria were not due to a reduction in the expression of MRC proteins, as the levels of MRCI, II, III, IV and V were similar in KO and WT mitochondria (n=6-8, data not shown), suggesting a posttranslational inactivation mechanism. Previous studies have reported that ROS, specifically H_2O_2, inhibit mitochondrial respiratory rates in rat liver cells (Corbisier et al., 1990), cardiomyocytes (Konno and Kako, 1992) and human megakaryocytic cells (Austin et. al., 1998). We report a similar effect in cortical mitochondria isolated from WT mice where acute application of H_2O_2 inhibited MRCI-driven respiration by 29±8% ($p<0.05$; Fig.1C). In KO mitochondria, the reduced MRCI-driven respiratory rates were associated with a 20±5% increase in H_2O_2 levels in cortex ($p<0.05$) and a 35±3% increase in hippocampus ($p<0.0001$; n=4-5; Fig.1D). Previous studies report H_2O_2-mediated inhibition of respiratory rates may be due to direct actions on MRCI (Ryan et al., 2012) or indirect actions via inhibiting aconitase and alpha-ketoglutarate dehydrogenase (Tretter and Adam-Vizi 2000; Starkov et al., 2004), key tricarboxylic acid cycle (TCA) enzymes upstream of MRCI substrate nicotinamide adenine dinucleotide (NADH) generation. In addition to reductions in TCA cycle enzyme and MRCI activity, antioxidant systems have been reported to be significantly reduced (including plasma vitamin C levels) and oxidative damage elevated in patients with epilepsy (Kunz et al., 2000; Mueller et al., 2001; Sudha et al., 2001; Malthankar-Phatak et al., 2006; Vielhaber et al., 2008).

Functional uncoupling is an inducible mechanism to protect against mitochondrial ROS formation (Sullivan et al., 2003; Sullivan et al., 2004; Andrews et al., 2005). In the brain, uncoupling protein 2 (UCP2) is the dominant protein that shuttles protons across the inner mitochondrial matrix in the presence of fatty acids, thereby uncoupling oxidation from ATP production and reducing the probability of electron spinoff and subsequent ROS formation (see Fig.1A). In epileptic KO mitochondria, UCP2 protein levels were reduced by 20±1% ($p<0.05$) and functional uncoupling was reduced by 68±1% when compared to WT values ($p<0.01$; Fig.1E), indicating a significant loss of function of the protein machinery that promotes successful electron transport. These data support our previous findings showing

that elevated H_2O_2 levels are associated with reduced mitochondrial uncoupling in adult rats exposed to KA seizures (Sullivan et al., 2003). Indeed, proactively preventing the formation of ROS, via enhancing functional uncoupling and reducing the existing ROS, have been proposed therapeutic strategies for epilepsy (Sullivan et al., 2003; Sullivan, 2005; Rowley and Patel, 2013, Kovac et al., 2012).

Whether MRCI impairment and the associated elevation in ROS enhances synchrony or promotes hyperexcitable neuronal networks remains unclear. Under normative concentrations, ROS act as small messenger molecules that facilitate synaptic plasticity (Thiels et al., 2000; Knapp and Klann, 2002; Kamsler and Segal, 2003a; Hongpaisan et al., 2004). However, at suprathreshold levels, ROS oxidize lipids, peptides and DNA, and alter synaptic transmission and plasticity (Kamsler and Segal, 2003b; Massaad and Klann, 2011). In cardiomyocytes, a mild increase in ROS acts as a signal to synchronize mitochondrial membrane potential oscillations throughout the cell; and these oscillations are associated with increasing action potential firing and excitability (Aon et al., 2003, 2006; Kurz et al., 2010). In terms of MRCI function, limited capacity of oxygen consumption due to reduced MRCI function is associated with less proton motive force available to drive ATP production at MRCV. Approximately 97% of ATP is produced by oxidative phosphorylation and neuronal mitochondria are strategically localized in regions of intense energy consumption, including dendrites and presynaptic axon terminals (Ligon and Steward, 2000; Harris et al., 2012). With the estimated cost of transmitting one bit of information to be 25,000 ATP molecules, pre- and post-synaptic events (including membrane repolarization by Na^+/ATPase and K^+/ATPases) consume an estimated 41% of the ATP pools (Ligon and Steward, 2000; Hall et al., 2012; Harris et al., 2012). Therefore, among potential consequences, a 30% reduction in ATP-producing respiratory rates may attenuate the cell's ability to fully repolarize, thus increasing neuronal excitability. Indeed, recent studies indicate that impairment of MRCI interferes with the ability of hippocampal networks to oscillate at specific frequencies (Kann et al., 2011; Harris et al., 2012).

MRCI impairment exacerbates provoked hippocampal hyperexcitability

We determined whether experimentally impairing mitochondria in WT hippocampal slices by reducing MRCI function with 100nM rotenone [a concentration known to elevate ROS (Li et al., 2003)] alters hippocampal excitability. We performed extracellular recordings and examined the mossy fiber-CA3 synapse, as it plays an important modulating role in CA3-generated epileptiform activity. Bath application of rotenone slightly increased the postsynaptic field potentials by 12±5% and decreased the paired pulse ratios (PPRs) by 20±4% ($p<0.001$, Fig.1F), suggesting increased release probabilities from mossy fibers. Previous studies indicate that presynaptic neurotransmitter release probabilities depend on mitochondrial functions, including ATP to support and regulate vesicular release and recycling (Billups and Forsythe, 2002; Guo et al., 2005; Chouhan et al., 2012).

To determine whether MRCI impairment influences seizure-like events (SLEs), rotenone was bath applied with high potassium (8mM)-containing aCSF, an *in vitro* model of epileptiform activity (Traynelis and Dingledine, 1988). The resultant SLEs had increased duration and frequency, as measured by inter-SLE intervals, compared to vehicle controls

(Fig.1G). We and others have shown similar reduced mossy fiber paired pulse facilitation and enhanced high potassium effects in KO hippocampal slices supporting the possibility that MRCI dysfunction may contribute to the mechanisms of hyperexcitability in KO mice (Simeone et al., 2013; Smart et al., 1998). These data further support the notion that impairment of mitochondrial function dynamically engages a negative feedforward cycle resulting in increased network excitability (Harris et al., 2012; Massaad and Klann, 2011; Cunningham et al., 2006; Kann et al., 2011; Sullivan et al., 2003; 2004; Kudin et al., 2009; Aon et al., 2003).

Daily treatment with AATP improves mitochondrial functions and mossy fiber-CA3 PPRs, and reduces seizure burden in KO mice

AATP was designed to enhance ATP-producing MRCI respiratory rates, functional uncoupling and antioxidant capacity. KO mice were treated daily with AATP and (i) mitochondrial functions, (ii) synaptic PPRs, and (iii) seizure incidence and severity were determined. AATP treatment significantly increased respiratory rates of cortical and hippocampal mitochondria (cortical data shown in Fig.2A. Hippocampal state III of AATP-treated KO: 231.3±22.4 vs. KO: 115.2±8.6 $nmol^{-1}mg^{-1}min^{-1}$; n=3-4). When compared to KO, ROS was reduced by 14±2% in cortex (1.66±0.07 vs. 1.46±0.03, $p<0.05$) and by 12±3% in the hippocampus (1.32±0.02 vs. 1.16±0.04, $p<0.01$; n=4-5) of AATP-treated KO mice. Functional uncoupling of AATP-treated KO mice did not differ from WT controls (cortex shown in Fig.2A. Hippocampus: AATP-treated KO: 2.4±0.4 vs. WT: 1.6±0.2). Similar to our previous report (Simeone et al., 2013), the KO field potential slopes were ~225±9% larger than WT and PPRs were 51% lower at the mossy fiber-CA3 synapses following paired-pulse stimulations (Fig.2B,C). *In vivo* AATP-treatment of KO mice restored the *in vitro* PPRs to WT levels (Fig.2B), however, treatment did not influence the field potential slopes (Fig.2C). Further examination of the normalized I/O relationships revealed that the KO V_{50} was 17% lower than the WT V_{50} (49.7±1.85μA vs. 59.6±2.56μA, $p<0.05$, n=4), and the AATP-treated KO V_{50} did not differ from WT (57±2.81μA, n=5; Fig. 2C). The restored PPRs and reduced V_{50} indicate that AATP-treatment decreases KO excitability and neurotransmitter release probabilities at the mossy fiber-CA3 synapses. However, the lack of an effect on the field potential slopes suggests that increased mossy fiber-CA3 synaptic responses occur via another mechanism, such as increased action potential duration. Future studies will examine this mechanism and determine whether it may contribute to the lack of complete seizure freedom in AATP-treated mice (see below).

To account for treatment stabilization (Fig.2D), SBI and seizure incidence were analyzed during the last two days of AATP treatment. Using intent-to-treat analyses, AATP treatment significantly reduced seizure burden index (SBI) scores in KO mice [$F(2,34)=4.7$; $p<0.05$ (Fig.2E)] when compared to baseline. The reduction persisted following cessation of treatment ($p<0.05$, compared to baseline) and was more apparent when compared to post-treatment age-matched control KO mice ($p<0.001$). To discern between effects on seizure severity and frequency, we analyzed the incidence among groups. The incidence of seizures was significantly less in AATP-treated KO mice when compared to baseline scores [$F(2,25)=4.9$; $p<0.05$]. This effect remained following cessation of treatment when compared to age-matched controls ($p<0.05$; Fig.2E). Overall, AATP treatment reduced SBI

by 51±8% in 7/9 subjects and incidence by 50±9% in 8/9 subjects. During the 48 hr treatment cessation phase, more than two-thirds of mice retained >50% reduction in SBI (69±7%) and incidence (73±8%) when compared to age-matched controls.

Ascorbic acid, alpha-tocopherol and pyruvate have either been used or considered for epilepsy therapy (Rowley and Patel, 2013, Kovac et al., 2012), however, when administered independently, preclinical and clinical studies have reported contradicting anti-seizure results (Ogunmekan and Hwang, 1989; Levy et al., 1992; Ayyildiz et al., 2007; Xu and Stinger, 2008). These studies combined with our data suggest that the synergistic mechanisms of actions of the combination treatment of AATP may enhance anti-seizure efficacy. Future studies will determine whether a longer treatment regiment will further normalize ROS levels, restore hippocampal network responses and completely abolish seizures in the KO mouse model of severe temporal lobe epilepsy.

Acute pretreatment with AATP to WT mice reduces severity of KA induced seizures

We have previously shown that reduced MRCI rates are associated with elevated ROS and reduced functional uncoupling in mitochondria isolated from adult rats following KA induced seizures (Sullivan et al., 2003). Therefore, we pretreated WT mice with either vehicle or AATP 30 min prior to KA injection to determine whether targeting mitochondrial functions *a priori* exerts anti-seizure effects. Electro-behavioral seizures were apparent within the first 30 min following KA administration in both groups of mice (Fig.2F). AATP pre-treatment did not influence the latency to onset of Stage 2 seizures. By 90 min, the entire vehicle-treated cohort experienced Stage 3-5 seizures. Xu and Stringer (2008) reported that when administered alone, tocopherol or ascorbic acid protected only 20% of mice from severe KA induced seizures (Stage 3-5). We found that pretreatment with AATP protected 100% of subjects from Stage 4-5 seizures. A two-factor mixed model ANOVA with repeated measures determined significant reductions of seizure severity in AATP-pretreated WT mice when compared to vehicle-treated controls [Treatment $F(1,8)=19.61$; $p<0.005$; Time $F(5,40)=3.77$; $p<0.01$; Fig.2G], specifically at 90, 150 and 180 min (Bonferroni multiple comparisons *post hoc* test, $p<0.05$). Previous studies report elevated ROS levels and MRCI impairment is apparent already by 3 hrs after KA-induced seizure onset and continues for at least 24 hrs (Chuang et al., 2009; Sullivan et al., 2003). Here, we show that MRCI impairment exacerbates the duration and frequency of seizure-like events *in vitro* (Fig.1G). Collectively, these data suggest that synergistic mechanisms of actions of AATP pretreatment may provide protection against the severe seizures induced by KA.

CONCLUSION

The primary results of this study are that (1) MRCI-driven respiratory and uncoupling rates are reduced and ROS is elevated in mitochondria of epileptic KO mice. (2) Experimental impairment of MRCI in WT hippocampal slices via rotenone reduces PPRs at mossy fiber-CA3 synapses, indicating increased neurotransmitter release probabilities, and exacerbates SLEs *in vitro*. (3) AATP treatment restores mitochondrial function, PPRs and attenuates seizure burden in KO mice. (4) AATP pretreatment results in 100% protection from severe KA-induced seizures in WT mice. Collectively, our data suggest active involvement of

pathologic mitochondria in temporal lobe epilepsy and support the development of therapies targeting the restoration of brain bioenergetic homeostasis.

Acknowledgments

The authors wish to thank the Nebraska LB692, Epilepsy Foundation of America and National Institutes of Health (NS072179) for funding this research. This project was also supported by Grant Number G20RR024001 from the National Center for Research Resources. The content is solely the responsibility of the authors and does not necessarily represent the official views of the national Center for Research Resources or the National Institutes of Health. Please note, the first author has published under the names KA Dorenbos, KA Fenoglio, KA Fenoglio-Simeone and KA Simeone.

ABBREVIATIONS

AATP	ascorbic acid, alpha-tocopherol, pyrvate
ADP	adenosine diphosphate
ATP	adenosine triphosphate
FA	fatty acid
FCCP	p-triflourometh-oxyphenylhydrazone
KA	kainic acid
KO	Kv1.1 knockout mice
MRC	mitochondrial respiratory complex
Oligo	oligomycin
P	postnatal day
PM	pyruvate and malate
PPR	paired pulse ratios
ROS	reactive oxygen species
Rot	rotenone
SBI	seizure burden index
SLE	seizure-like event
TCA	tricarboxylic acid
UCP2	uncoupling protein 2
WT	wild-type

REFERENCES

Andrews ZB, Diano S, Horvath TL. Mitochondrial uncoupling proteins in the CNS: in support of function and survival. Nat. Rev. Neurosci. 2005; 6:829–840. [PubMed: 16224498]

Aon MA, Cortassa S, Marbán E, O'Rourke B. Synchronized whole cell oscillations in mitochondrial metabolism triggered by a local release of reactive oxygen species in cardiac myocytes. J. Biol. Chem. 2003; 278:44735–44744. [PubMed: 12930841]

Aon MA, Cortassa S, O'Rourke B. The fundamental organization of cardiac mitochondria as a network of coupled oscillators. Biophys J. 2006; 91:4317–427. [PubMed: 16980364]

Austin RC, Sood SK, Dorward AM, Singh G, Shaughnessy SG, Pamidi S, Outinen PA, Weitz JI. Homocysteine-dependent alterations in mitochondrial gene expression, function and structure. Homocysteine and H2O2 act synergistically to enhance mitochondrial damage. J. Biol. Chem. 1998; 273:30808–30817. [PubMed: 9804859]

Ayyildiz M, Coskun S, Yildirim M, Agar E. The effects of ascorbic acid on penicillin-induced epileptiform activity in rats. Epilepsia. 2007; 48:1388–1395. [PubMed: 17433052]

Billups B, Forsythe ID. Presynaptic mitochondrial calcium sequestration influences transmission at mammalian central synapses. J Neurosci. 2002; 22:5840–5847. [PubMed: 12122046]

Brown MR, Sullivan PG, Dorenbos KA, Modafferi EA, Geddes JW, Steward O. Nitrogen disruption of synaptoneurosomes: an alternative method to isolate brain mitochondria. J. Neurosci. Methods. 2004; 137:299–303. [PubMed: 15262074]

Bruce AJ, Baudry M. Oxygen free radicals in rat limbic structures after kainate-induced seizures. Free Radic Biol Med. 1995; 18:993–1002. [PubMed: 7628735]

Chaudière J, Ferrari-Iliou R. Intracellular Antioxidants: from Chemical to Biochemical Mechanisms Food and Chemical Toxicology. 1999; 37:949–962.

Chouhan AK, Ivannikov MV, Lu Z, Sugimori M, Llinas RR, Macleod GT. Cytosolic calcium coordinates mitochondrial energy metabolism with presynaptic activity. J. Neurosci. 2012; 32:1233–1243. [PubMed: 22279208]

Chuang YC, Chen SD, Liou CW, Lin TK, Chang WN, Chan SH, Chang AY. Contribution of nitric oxide, superoxide anion, and peroxynitrite to activation of mitochondrial apoptotic signaling in hippocampal CA3 subfield following experimental temporal lobe status epilepticus. Epilepsia. 2009; 50:731–46. [PubMed: 19178557]

Corbisier P, Raes M, Michiels C, Pigeolet E, Houbion A, Delaive E, Remacle J. Respiratory activity of isolated rat liver mitochondria following in vitro exposure to oxygen species: a threshold study. Mech. Ageing Dev. 1990; 51:249–63. [PubMed: 2308396]

Cunningham MO, Pervouchine DD, Racca C, Kopell NJ, Davies CH, Jones RS, Traub RD, Whittington MA. Neuronal metabolism governs cortical network response state. Proc. Natl. Acad. Sci. U. S. A. 2006; 103:5597–5601. [PubMed: 16565217]

DiMauro S, Kulikova R, Tanji K, Bonilla E, Hirano M. Mitochondrial genes for generalized epilepsies. Adv. Neurol. 1999; 79:411–419. [PubMed: 10514830]

Fenoglio-Simeone KA, Wilke JC, Milligan HL, Allen CN, Rho JM, Maganti RK. Ketogenic diet treatment abolishes seizure periodicity and improves diurnal rhythmicity in epileptic Kcna1-null mice. Epilepsia. 2009; 50:2027–2034. [PubMed: 19490051]

Guo X, Macleod GT, Wellington A, Hu F, Panchumarthi S, Schoenfield M, Marin L, Charlton MP, Atwood HL, Zinsmaier KE. The GTPase dMiro is required for axonal transport of mitochondria to Drosophila synapses. Neuron. 2005; 47:379–393. [PubMed: 16055062]

Hall CN, Klein-Flügge MC, Howarth C, Attwell D. Oxidative phosphorylation, not glycolysis, powers presynaptic and postsynaptic mechanisms underlying brain information processing. J Neurosci. 2012; 32:8940–8951. [PubMed: 22745494]

Harris JJ, Jolivet R, Attwell D. Synaptic energy use and supply. Neuron. 2012; 75:762–777. [PubMed: 22958818]

Hongpaisan J, Winters CA, Andrews SB. Strong calcium entry activates mitochondrial superoxide generation, upregulating kinase signaling in hippocampal neurons. J. Neurosci. 2004; 24:10878–10887. [PubMed: 15574738]

Jarrett SG, Liang LP, Hellier JL, Staley KJ, Patel M. Mitochondrial DNA damage and impaired base excision repair during epileptogenesis. Neurobiol Dis. 2008; 30:130–138. [PubMed: 18295498]

Kamsler A, Segal M. Hydrogen peroxide modulation of synaptic plasticity. J Neurosci. 2003a; 23:269–276. [PubMed: 12514224]

Kamsler A, Segal M. Paradoxical actions of hydrogen peroxide on long-term potentiation in transgenic superoxide dismutase-1 mice. J Neurosci. 2003b; 23:10359–10367.

Kann O, Huchzermeyer C, Kovács R, Wirtz S, Schuelke M. Gamma oscillations in the hippocampus require high complex I gene expression and strong functional performance of mitochondria. Brain. 2011; 134:345–358. [PubMed: 21183487]

Knapp LT, Klann E. Potentiation of hippocampal synaptic transmission by superoxide requires the oxidative activation of protein kinase C. J. Neurosci. 2002; 22:674–683. [PubMed: 11826097]

Konno N, Kako KJ. Role of cellular defense against hydrogen peroxide-induced inhibition of myocyte respiration. Basic Res. Cardiol. 1992; 87:239–49. [PubMed: 1520249]

Kovac S, Abramov AY, Walker MC. Energy depletion in seizures: Anaplerosis as a strategy for future therapies. Neuropharmacology. 2013; 69:96–104. [PubMed: 22659085]

Kudin AP, Zsurka G, Elger CE, Kunz WS. Mitochondrial involvement in temporal lobe epilepsy. Exp. Neurol. 2009; 218:326–332. [PubMed: 19268667]

Kunz WS, Kudin AP, Vielhaber S, Blümcke I, Zuschratter W, Schramm J, Beck H, Elger CE. Mitochondrial complex I deficiency in the epileptic focus of patients with temporal lobe epilepsy. Ann Neurol. 2000; 48:766–773. [PubMed: 11079540]

Kurz FT, Aon MA, O'Rourke B, Armoundas AA. Spatio-temporal oscillations of individual mitochondria in cardiac myocytes reveal modulation of synchronized mitochondrial clusters. Proc. Natl. Acad. Sci. 2010; 107:14315–14320. [PubMed: 20656937]

Levy SL, Burnham WM, Bishai A, Hwang PA. The anticonvulsant effects of vitamin E: a further evaluation. Can J Neurol Sci. 1992; 19:201–203. [PubMed: 1623446]

Li N, Ragheb K, Lawler G, Sturgis J, Rajwa B, Melendez JA, Robinson JP. Mitochondrial complex I inhibitor rotenone induces apoptosis through enhancing mitochondrial reactive oxygen species production. J Biol Chem. 2003; 278:8516–8525. [PubMed: 12496265]

Lian XY, Khan FA, Stringer JL. Fructose-1,6-bisphosphate has anticonvulsant activity in models of acute seizures in adult rats. J Neurosci. 2007; 27:12007–12011. [PubMed: 17978042]

Ligon LA, Steward O. Movement of mitochondria in the axons and dendrites of cultured hippocampal neurons. J. Comp. Neurol. 2000; 427:340–350. [PubMed: 11054697]

Malthankar-Phatak GH, de Lanerolle N, Eid T, Spencer DD, Behar KL, Spencer SS, Kim JH, Lai JC. Differential glutamate dehydrogenase (GDH) activity profile in patients with temporal lobe epilepsy. Epilepsia. 2006; 47:1292–1299. [PubMed: 16922873]

Massaad CA, Klann E. Reactive oxygen species in the regulation of synaptic plasticity and memory. Antioxid. Redox Signal. 2011; 14:2013–54. [PubMed: 20649473]

Mueller SG, Kollias SS, Trabesinger AH, Buck A, Boesiger P, Wieser HG. Proton magnetic resonance spectroscopy characteristics of a focal cortical dysgenesis during status epilepticus and in the interictal state. Seizure. 2001; 10:518–524. [PubMed: 11749111]

Munteanu A, Taddei M, Tamburini I, Bergamini E, Azzi A, Zingg JM. Antagonistic effects of oxidized low density lipoprotein and alpha-tocopherol on CD36 scavenger receptor expression in monocytes: involvement of protein kinase B and peroxisome proliferator-activated receptor-gamma. J. Biol. Chem. 2006; 281:6489–6497. [PubMed: 16407258]

Ogunmekan AO, Hwang PA. A randomized, double-blind, placebo-controlled, clinical trial of D-alpha-tocopheryl acetate (vitamin E), as add-on therapy, for epilepsy in children. Epilepsia. 1989; 30:84–89. [PubMed: 2643513]

Rowley S, Patel M. Mitochondrial involvement and oxidative stress in temporal lobe epilepsy. Free Radic. Biol. Med. 2013 doi:pii: S0891-5849(13)00055-5.10.1016/j.freeradbiomed.2013.02.002.

Ryan K, Backos DS, Reigan P, Patel M. Post-translational oxidative modification and inactivation of mitochondrial complex I in epileptogenesis. J Neurosci. 2012; 32:11250–11258. [PubMed: 22895709]

Simeone KA, Sabesan S, Kim, do Y, Kerrigan JF, Rho JM, Simeone TA. L-Type calcium channel blockade reduces network activity in human epileptic hypothalamic hamartoma tissue. Epilepsia. 2011; 52(3):531–540. [PubMed: 21269296]

Simeone TA, Simeone KA, Samson KK, Kim DY, Rho JM. Loss of the Kv1.1 potassium channel promotes pathologic sharp waves and high frequency oscillations in in vitro hippocampal slices. Neurobiol. Dis. 2013; 54C:68–81. [PubMed: 23466697]

Smart SL, Lopantsev V, Zhang CL, Robbins CA, Wang H, Chiu SY, Schwartzkroin PA, Messing A, Tempel BL. Deletion of the K(V)1.1 potassium channel causes epilepsy in mice. Neuron. 1998; 20:809–819. [PubMed: 9581771]

Sudha K, Rao AV, Rao A. Oxidative stress and antioxidants in epilepsy. Clin Chim Acta. 2001; 303:19–24. [PubMed: 11163018]

Sullivan PG, Dubé C, Dorenbos KA, Steward O, Baram TZ. Mitochondrial uncoupling protein-2 protects the immature brain from excitotoxic neuronal death. Ann. Neurol. 2003; 53:711–717. [PubMed: 12783416]

Sullivan PG, Rippy NA, Dorenbos K, Concepcion RC, Agarwal AK, Rho JM. The ketogenic diet increases mitochondrial uncoupling protein levels and activity. Ann. Neurol. 2004; 55:576–580. [PubMed: 15048898]

Sullivan PG. Interventions with neuroprotective agents: novel targets and opportunities. Epilepsy Behav. 2005; 7:S12–17. [PubMed: 16239125]

Starkov AA, Fiskum G, Chinopoulos C, Lorenzo BJ, Browne SE, Patel MS, Beal MF. Mitochondrial alpha-ketoglutarate dehydrogenase complex generates reactive oxygen species. J. Neurosci. 2004; 24:7779–7788. [PubMed: 15356189]

Thiels E, Urban NN, Gonzalez-Burgos GR, Kanterewicz BI, Barrionuevo G, Chu CT, Oury TD, Klann E. Impairment of long-term potentiation and associative memory in mice that overexpress extracellular superoxide dismutase. J Neurosci. 2000; 20:7631–7639. [PubMed: 11027223]

Traynelis SF, Dingledine R. Potassium-induced spontaneous electrographic seizures in the rat hippocampal slice. J Neurophysiol. 1988; 59:259–276. [PubMed: 3343603]

Tretter L, Adam-Vizi V. Inhibition of Krebs cycle enzymes by hydrogen peroxide: A key role of [alpha]-ketoglutarate dehydrogenase in limiting NADH production under oxidative stress. J. Neurosci. 2000; 20:8972–8979. [PubMed: 11124972]

Vielhaber S, Niessen HG, Debska-Vielhaber G, Kudin AP, Wellmer J, Kaufmann J, Schönfeld MA, Fendrich R, Willker W, Leibfritz D, Schramm J, Elger CE, Heinze HJ, Kunz WS. Subfield-specific loss of hippocampal N-acetyl aspartate in temporal lobe epilepsy. Epilepsia. 2008; 49:40–50. [PubMed: 17822430]

Wallace DC. Mitochondrial genetics: a paradigm for aging and degenerative diseases? Science. 1992; 256:628–632. [PubMed: 1533953]

Wenzel HJ, Vacher H, Clark E, Trimmer JS, Lee AL, Sapolsky RM, Tempel BL, Schwartzkroin PA. Structural consequences of Kcna1 gene deletion and transfer in the mouse hippocampus. Epilepsia. 2007; 48:2023–2046. [PubMed: 17651419]

Wu JS, Lin TN, Wu KK. Rosiglitazone and PPAR-gamma overexpression protect mitochondrial membrane potential and prevent apoptosis by upregulating anti-apoptotic Bcl-2 family proteins. J. Cell. Physiol. 2009; 220:58–71. [PubMed: 19229877]

Xu K, Stringer JL. Antioxidants and free radical scavengers do not consistently delay seizure onset in animal models of acute seizures. Epilepsy Behav. 2008; 13:77–82. [PubMed: 18396108]

Yonutas HM, Sullivan PG. Targeting PPAR Isoforms Following CNS Injury. Curr Drug Targets. 2013; 14:733–742. [PubMed: 23627890]

HIGHLIGHTS

- MRCI-driven respiratory and uncoupling rates are reduced and ROS is elevated in mitochondria isolated from epileptic Kv1.1 knockout (KO) mice.
- Experimental impairment of MRCI in WT hippocampal slices via rotenone reduces paired-pulse ratios at mossy fiber-CA3 synapses, indicating increased neurotransmitter release probabilities, and exacerbates SLEs *in vitro*.
- Daily AATP treatment restores mitochondrial function, mossy fiber paired-pulse ratios and attenuates seizure development resulting in a greater than 50% reduction of seizure burden index (SBI) scores in more than two-thirds of KO mice.
- AATP pretreatment results in 100% protection from severe KA-induced seizures in WT mice.
- These findings underscore the importance of mitochondria in network homeostasis and support mitochondria as a viable target for therapeutic development.

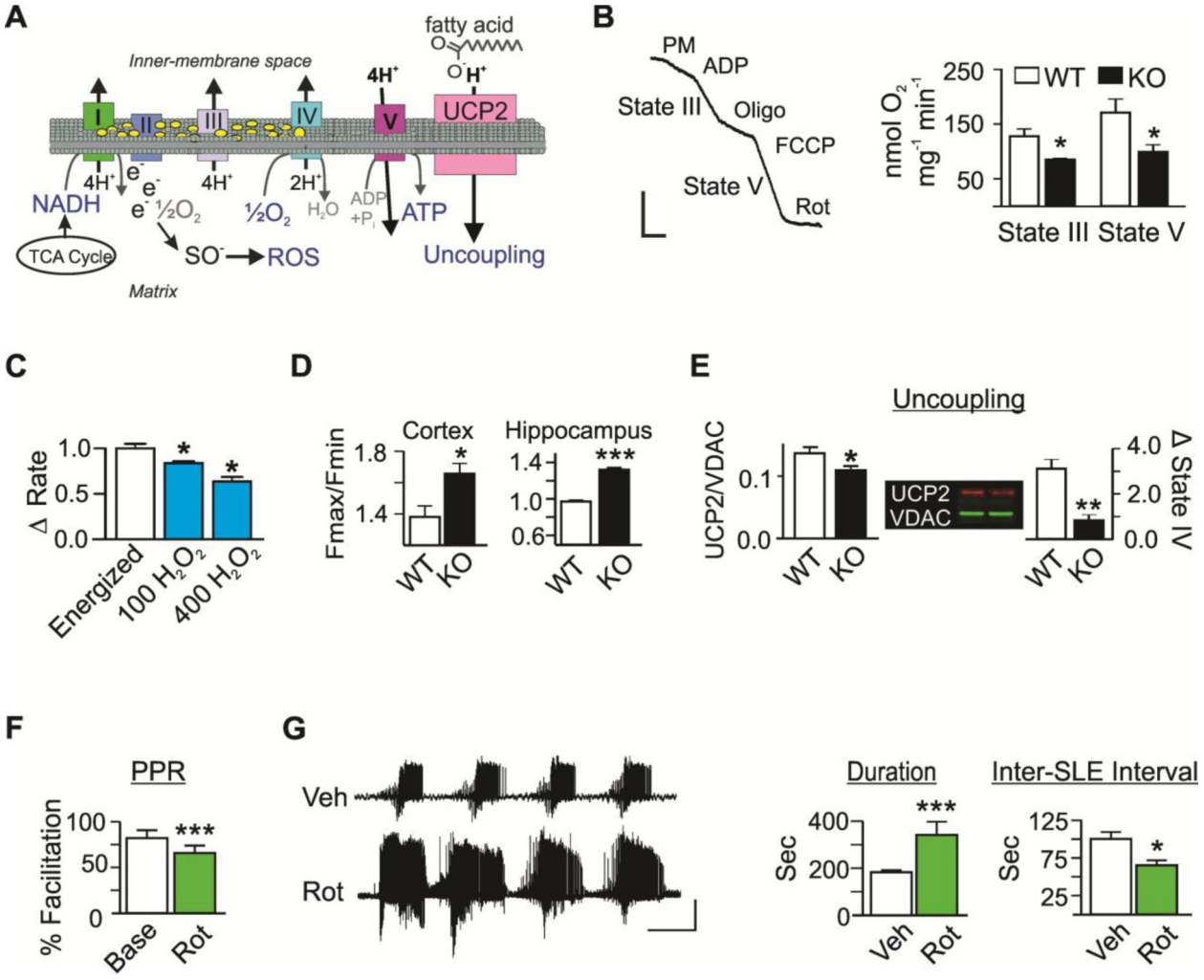

Figure 1. Impairment of mitochondrial functions is associated with epilepsy *in vivo* and hyperexcitable hippocampal circuitry *in vitro*

(A) Schematic depicting oxidative phosphorylation, the binding of free electrons to molecular oxygen to form ROS, and fatty acid-mediated proton transport thru uncoupling protein (UCP) 2. **(B)** Raw WT oxygen polarographic trace illustrating respiratory rates and quantification of state III and V respiratory rates by WT (white) and KO (black) cortical mitochondria. Bars: 25 nmol O_2 min $^{-1}$ × 50 sec (n=5-7) **(C)** The change in stabilized state III respiration following sequential application of 100 and 400 μM H_2O_2 to energized WT mitochondria (n=3). **(D)** H_2O_2 levels of energized cortical and hippocampal mitochondria expressed as a ratio of relative fluorescent units (Fmax/Fmin) (n=3-5). **(E)** *Left:* Densimetric values of UCP2 protein immunofluorescent labeling normalized to VDAC in isolated mitochondria (n=6). *Right:* Functional uncoupling following application of free fatty acids (FA) to energized mitochondria in state IV was calculated as the percent increase in oxygen consumption (n=3-4). **(F)** Paired-pulse ratios (PPR) at baseline (Base, white) and following rotenone (Rot, green; n=6-7 slices, 6-7 mice). **(G)** Representative traces and quantification of extracellular CA3 SLE duration and Inter-SLE intervals in hippocampal slices following

application of vehicle (Veh, white) or Rot (n=3-7 slices, 3-7 mice). Bars: 0.5mV × 5min. Data are expressed as the mean ± SEM, *p<0.05, **p<0.01, ***p<0.001.

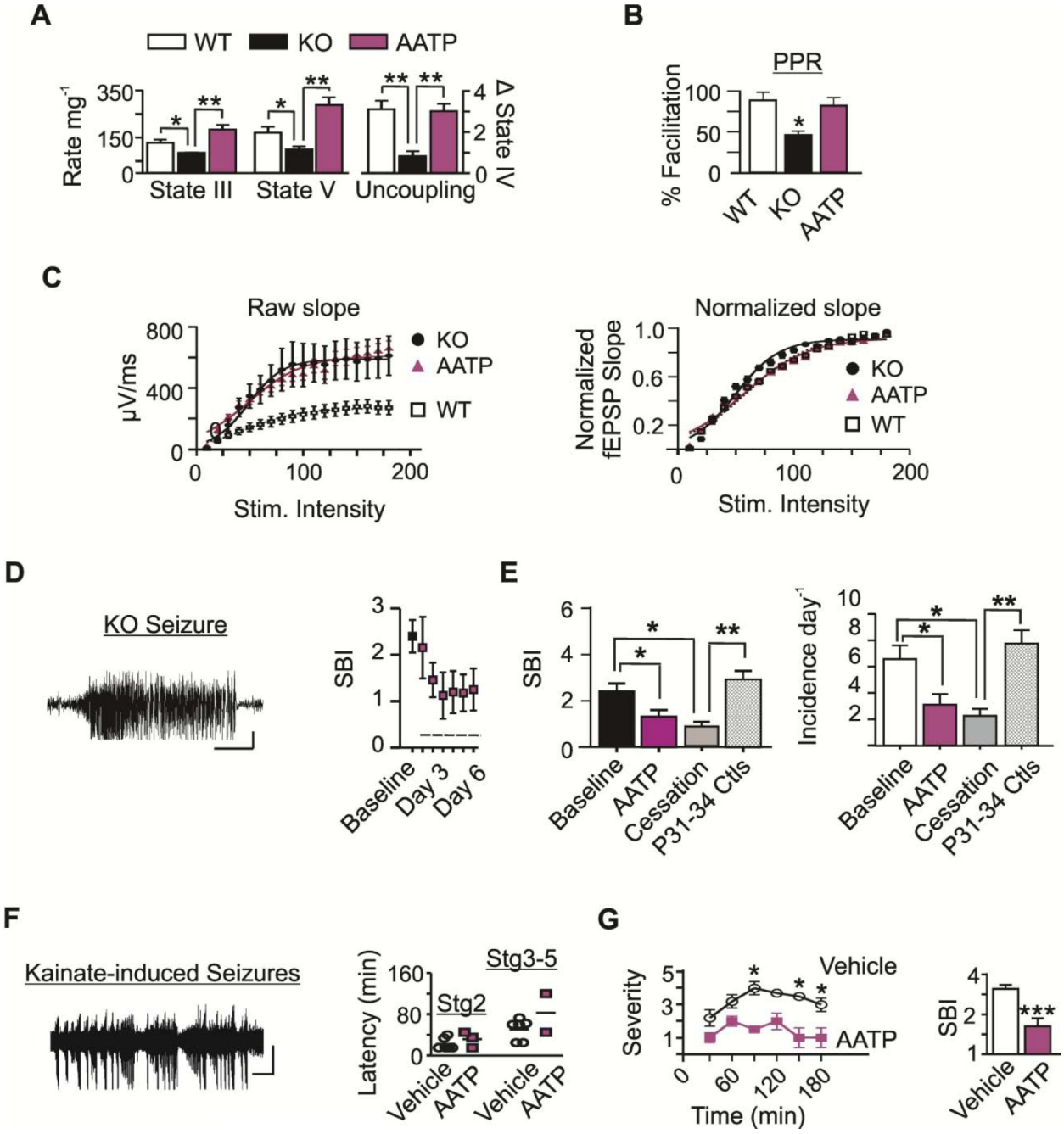

Figure 2. AATP treatment improves mitochondrial functions, PPRs and reduces seizure severity

(A) State III and V respiratory rates and functional uncoupling in KO mice treated with AATP (n=3-4). WT and KO data are replotted. **(B)** Paired-pulse (PP) facilitation (n=4-6) and **(C)** field potential slopes of WT (white), KO (black) and AATP-treated KO mice (magenta) (n=4-5). Field potential slope values are presented as (Left) raw and (Right) following I/O normalization across stimulation intensities. **(D)** KO Cortical EEG trace depicting ictal spike-wave discharges associated with a Stage 5 seizure. Bars: 200μV × 10 sec. SBI at baseline and during each day of treatment (indicated by the dashed line, n=9). **(E)** SBI at P21-P24 baseline (black, n=13), during the last two days of treatment (magenta,

n=9), and following cessation of treatment (grey, n=6); and in a cohort of age-matched controls (striped, n=4). **(F)** Spike-wave EEG discharges associated with Stage 3 and 4 behavioral seizures. Scatterplot depicting the latency to onset in those that experienced Stage 2 and Stage 3-5 seizures (n=4-6). Bars: 250μV × 50s. **(G)** Line graph of the mean severity at each epoch (collapsed across animals) and SBI scores (collapsed across time) (n=4-6). Data are expressed as the mean ± SEM, *p<0.05, **p<0.01, ***p<0.001.